

Molecular details of the unique mechanism of chloride transport by a cyanobacterial rhodopsin

Andrew Harris,^a Mattia Saita,^b Tom Resler,^b Alexandra Hughes-Visentin,^a Raiza Maia,^b Franziska Sellnau,^b Ana-Nicoleta Bondar,^c Joachim Heberle^{b*} and Leonid S. Brown^{a*}

^a Department of Physics and Biophysics Interdepartmental Group, University of Guelph, 50 Stone Road East, Guelph, Ontario N1G 2W1, Canada

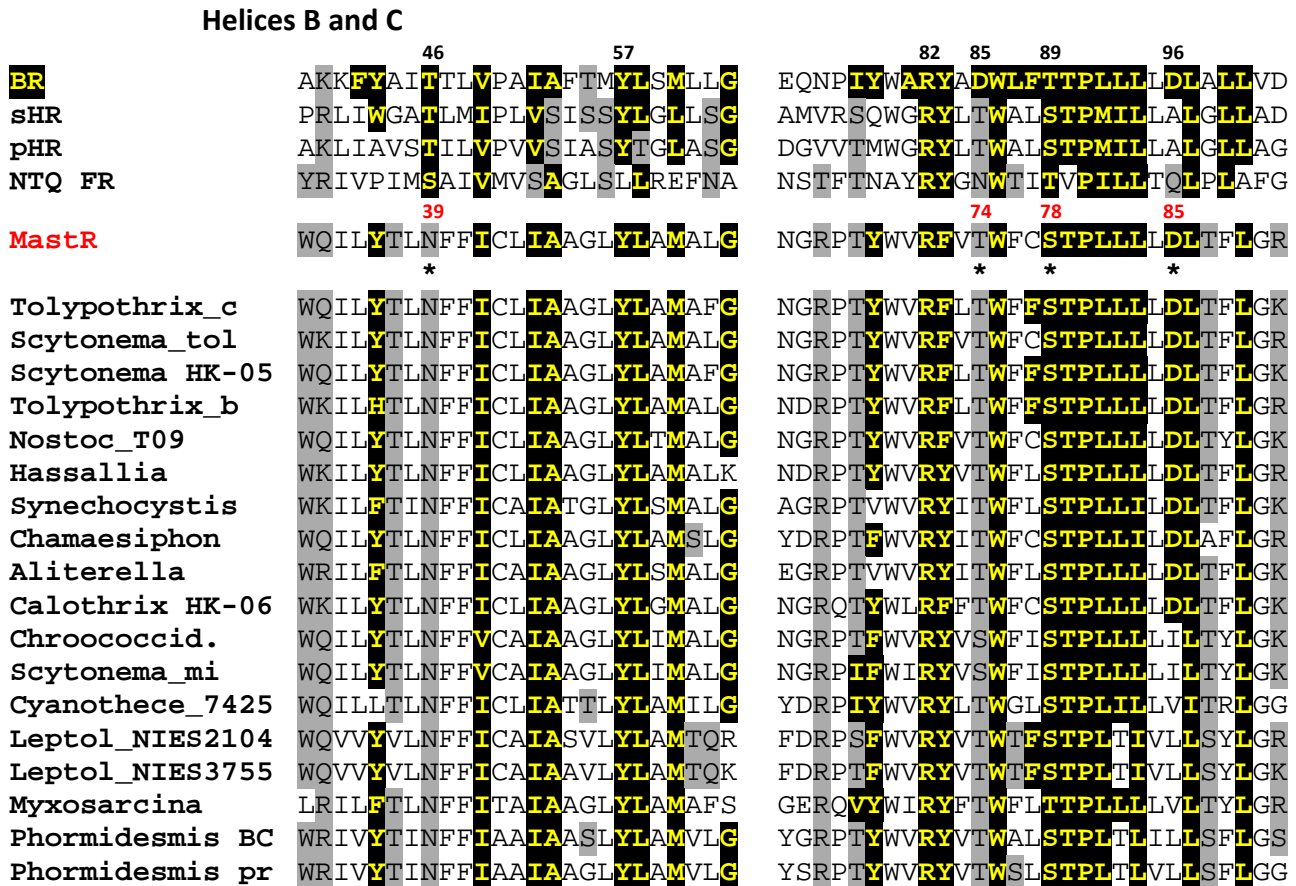
^b Experimental Molecular Biophysics Group, Department of Physics, Freie Universität Berlin, Arnimallee 14, 14195 Berlin, Germany

^c Theoretical Molecular Biophysics Group, Department of Physics, Freie Universität Berlin, Arnimallee 14, 14195 Berlin, Germany

Electronic Supplementary Information (ESI)

1. Supplementary figures

Figure S1. Sequence alignment for helices B-G for the cyanobacterial anion pumps and selected microbial rhodopsins. BR numbering is shown on top, MastR numbering shown in red. Asterisks show the mutation sites used in this work. Residues conserved in BR are shown in yellow on black, polar residues potentially involved in coordination of chloride in any group of chloride pumps are highlighted in grey. Abbreviations: BR – *Halobacterium salinarum* bacteriorhodopsin, sHR – *Halobacterium salinarum* halorhodopsin, pHR – *Natronobacterium pharaonis* halorhodopsin, NTQ FR – *Fulvimarina pelagi* NTQ rhodopsin, MastR – *Mastigocladopsis repens* rhodopsin, Tolypothrix_c – *Tolypothrix campylonemoides* rhodopsin, Scytonema_tol – *Scytonema tolypothrichoides* rhodopsin, Scytonema HK-05 – *Scytonema* sp. HK-05 rhodopsin, Tolypothrix_b – *Tolypothrix bouteillei* rhodopsin, Nostoc_T09 – *Nostoc* sp. T09 rhodopsin; Hassallia – *Hassallia bysoidea* rhodopsin, Synechocystis – *Synechocystis* sp. PCC 7509 rhodopsin, Chamaesiphon – *Chamaesiphon* sp. PCC 6605 rhodopsin, Aliterella – *Aliterella atlantica* rhodopsin, Calothrix HK-06 – *Calothrix* sp. HK-06 rhodopsin, Chroococcid. – *Chroococcidiopsis thermalis* rhodopsin, Scytonema_mi – *Scytonema millei* rhodopsin, Cyanothece_7425 – *Cyanothece* sp. PCC 7425 rhodopsin, Leptol_NIES2104 – *Leptolyngbya* sp. NIES-2104 rhodopsin, Leptol_NIES3755 – *Leptolyngbya* sp. NIES-3755 rhodopsin, Myxosarcina – *Myxosarcina* sp. G11 rhodopsin, Phormidesmis BC – *Phormidesmis* sp. BC1401 GrIS rhodopsin; Phormidesmis pr. – *Phormidesmis priestleyi*. The sequences are taken from public databases: NCBI Proteins and DOE JGI IMG.



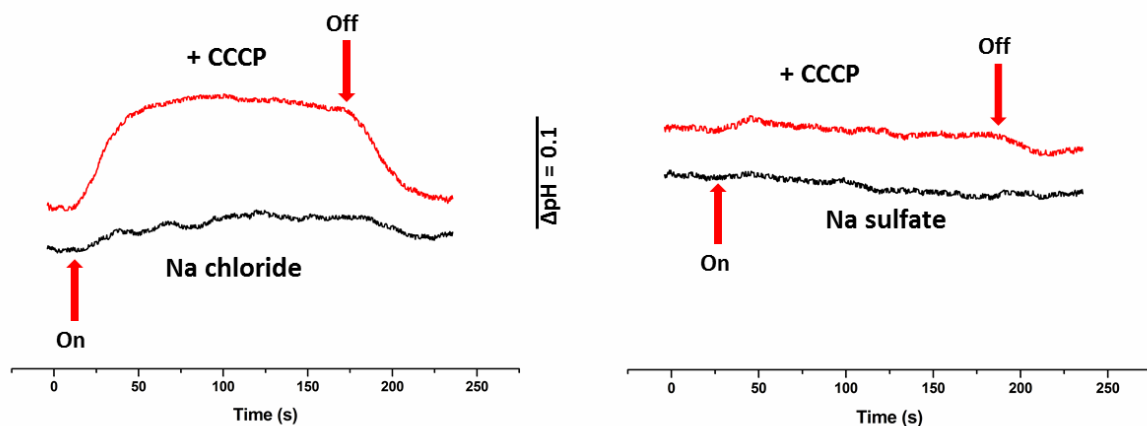


Figure S2. Chloride transport assays using whole *E. coli* cells expressing MastR suspended either in unbuffered 50 mM NaCl (left) or Na₂SO₄ (right), with and without 10 μM CCCP (proton uncoupler). pH changes were measured by glass electrode, the arrows show the time of turning yellow (570-590 nm) illumination on and off. See supplementary methods below for the full description.

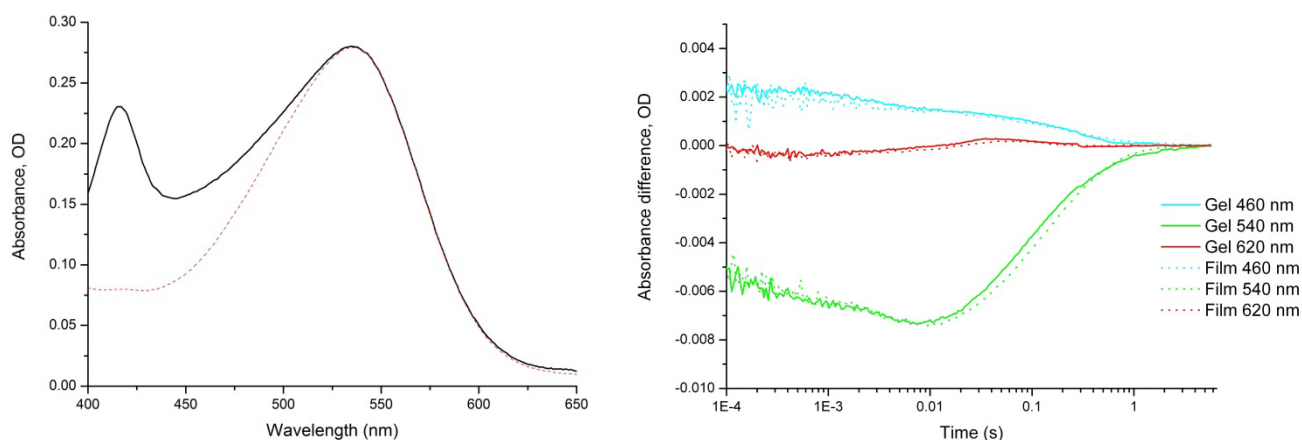


Figure S3. (Left) Absorption spectrum of the polyacrylamide-encased membranes of *E. coli* expressing MastR (black solid line) measured at pH 6, buffered by 0.05 M KH₂PO₄ and 0.05 M MES, at 22°C, with 2.5 M NaCl. Spectrum of the purified DDM-solubilized MastR (0.02 M NaCl, 0.05 M MES and 0.05 M KH₂PO₄, pH 6, 0.05% DDM) is given for comparison (red dashed line). **(Right)** Comparison of the photocycle kinetics of the polyacrylamide-encased membranes of *E. coli* expressing MastR and hydrated films of the same membranes, measured at pH 6, buffered by 0.05 M KH₂PO₄ and 0.05 M MES, at 22°C, with 0.02 M NaCl.

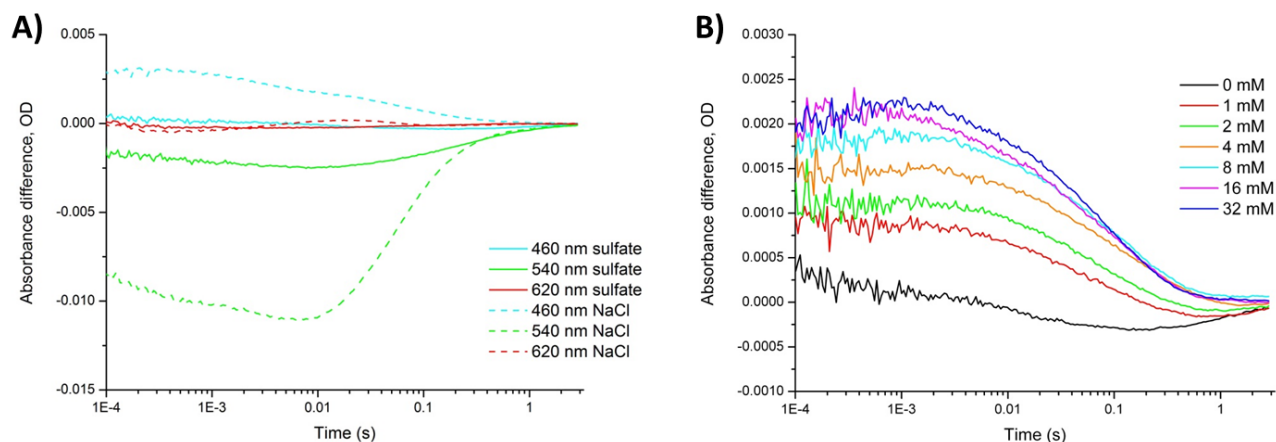


Figure S4. **A)** Comparison of chloride-transporting and chloride-free photocycles of MastR in *E. coli* membranes encased in polyacrylamide gels, measured at pH 6, buffered by 0.05 M KH_2PO_4 and 0.05 M MES, at 22°C, with either 0.1 M NaCl or 0.1 M Na_2SO_4 . **B)** Verification of the chloride binding affinity of the dark state of MastR by chloride titration of the amplitude of the 460 nm signal (the L/N intermediates) of the MastR photocycle. The specified sodium chloride concentrations (from 4 M stock) were added on top of 0.1 M Na_2SO_4 , other conditions are as in A).

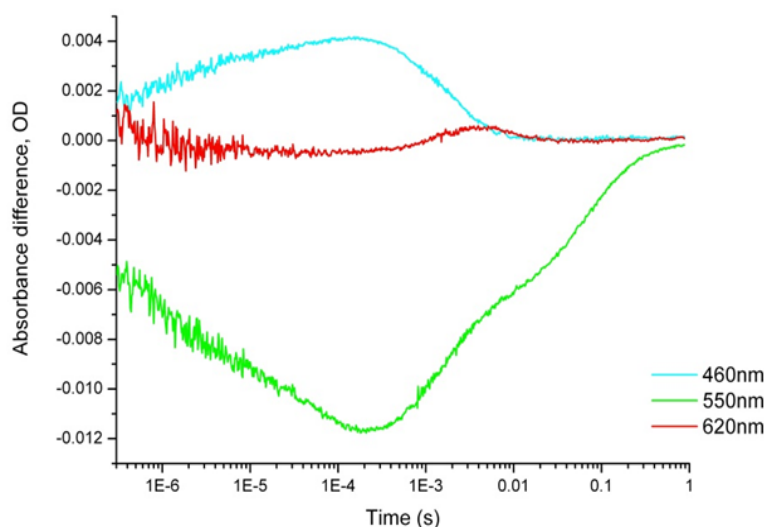


Figure S5. The photocycle of lipid-reconstituted MastR in proteoliposome film (DMPC/ DMPA 9/1) measured at 22°C, pH 6 (buffered by MES) and ~3 M KCl, used for the time-resolved infrared spectroscopy experiments. The buffer and salt concentrations are approximate due to the film drying effects (see Experimental).

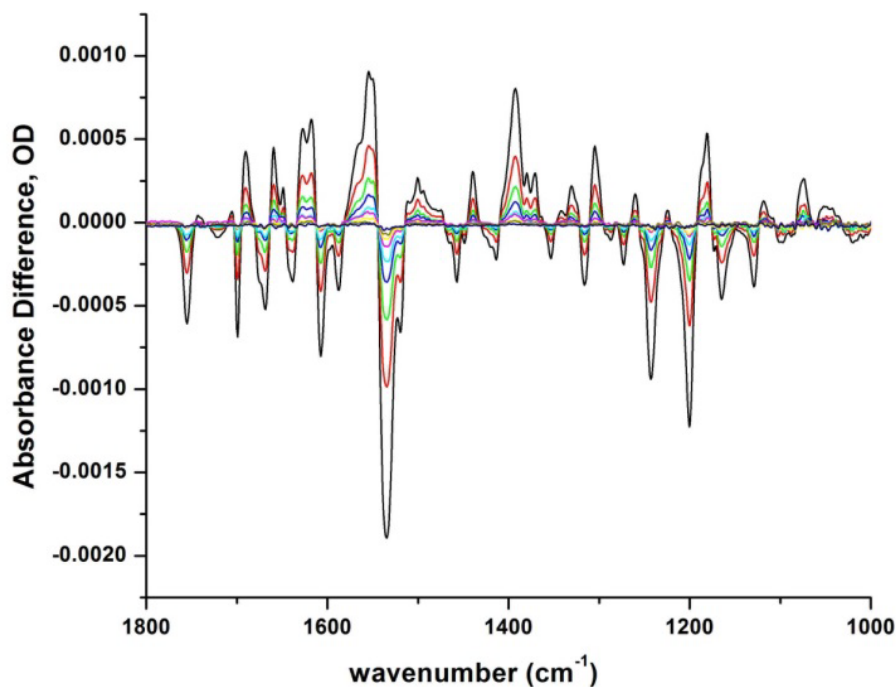


Figure S6. Rapid-scan (29 ms time resolution) light-minus-dark difference FTIR spectra of MastR proteoliposomes (sample conditions as in Fig. S5). Spectral resolution is 2 cm^{-1} , average of 6000 individual spectra. The black spectrum with the largest amplitude corresponds to 29 ms after the photoexcitation, and the other spectra represent relaxation of that state recorded every $\sim 74\text{ ms}$.

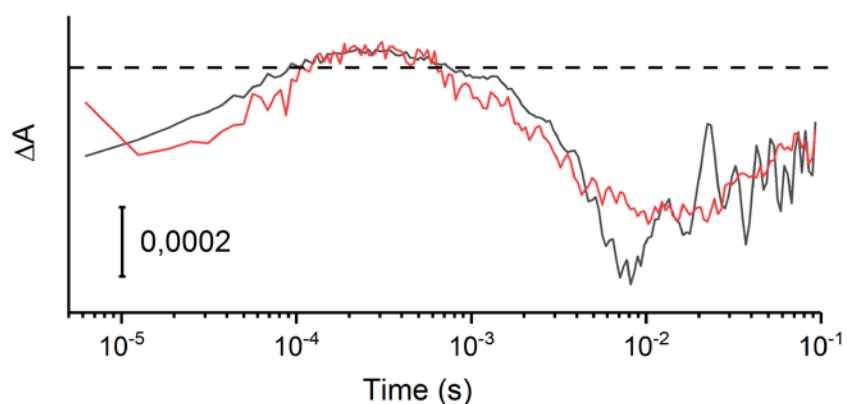


Figure S7. Kinetics of the amide I vibration at 1670 cm^{-1} measured with step-scan FTIR. The evolution of the conformational changes of the sample in H_2O (data from Fig. 8, black) compared to that in D_2O (red). The better signal-to-noise ratio in the late ms time range of the D_2O data is due to the lower absorption of the D_2O sample in this range.

2. Supplementary methods

2.1. Ion transport assays

Ion transport assays for MastR in the whole *E. coli* cells were performed according to the published protocol.¹ The cells from 1 L culture grown as described in the main text were collected at 4680 ×g and 4 °C for 10 min. Half of the cells were washed three times with unbuffered solution (50 mM NaCl, 10 mM MgSO₄·7H₂O, 100 μM CaCl₂), and then re-suspended for ion transport measurements. The other half were washed and resuspended similarly with chloride-free unbuffered solution (50 mM Na₂SO₄, 10 mM MgSO₄·7H₂O, 100 μM CaCl₂). A glass electrode (Accumet Microprobe Extra Long Calomel Combo Electrode) was used to monitor pH changes of the cells suspended in unbuffered solution with gentle stirring. A digital oscilloscope (Agilent Technologies DSO 1052B Digital Storage Oscilloscope) was used for recording the pH. The sample was illuminated (Cole Parmer 9741-50 illuminator) with yellow light (570–590 nm) using a glass filter.

2.2. Structure modeling

A homology model of MastR was derived using Modeller 19.9^{2,3} and the crystal structure of halorhodopsin PDB ID:1E12.⁴ During homology modeling, the retinal molecule and the chloride ion bound to the active site of HR were treated as ligand molecules and modeled into MastR. A total of 20 homology models were generated, and the structure with the lowest DOPE score (Discrete Optimized Protein Energy)⁵ was used for further optimization using the CHARMM software,⁶ as follows.

Coordinates for hydrogen atoms were generated using CHARMM with the all-atom c36 parameters for protein groups^{7,8} and the retinal force field parameters described earlier.⁹⁻¹¹ Inspection of the homology model of MastR indicated that the C₁₅=N bond twist was ~64°, as compared to -160.3° in the template structure of HR; this discrepancy could be due to limitations of the homology modeling software in describing the geometry and interactions of the retinal polyene chain. To circumvent this issue, we subjected the homology model of MastR to constrained geometry optimizations with CHARMM whereby we first drove the C₁₄-C₁₅=N-Cε dihedral angle to ~174°, and then performed a new geometry optimization with the dihedral angle constraint switched off. During both CHARMM geometry optimizations, backbone heavy atoms were fixed to their starting coordinates; non-bonded interactions were smoothly switched off using an atom-based switch function between 10Å and 12Å. In the resulting geometry-optimized structure of MastR, retinal is all-*trans* with C₁₃=C₁₄ and C₁₅=N bond twists of ~19° and ~2°, respectively.

A caveat of the current structure analysis of MastR is that according to tests using the Phyre2 server¹² the sequence identity between the MastR sequence and the sHR structure used as a template⁴ is somewhat low, ~27%. As observed when modelling channelrhodopsins using bacteriorhodopsin as a template,¹³ the relatively low level of sequence identity means that details of the MastR structural model might be inaccurate. In spite of this caveat, the geometry-optimized homology model used here suffices to derive clues about potential intra- and inter-helical interactions of protein groups known to be important for function.

3. Supplementary references

1. W. W. Wang, O. A. Sineshchekov, E. N. Spudich and J. L. Spudich, *J Biol Chem*, 2003, **278**, 33985-33991.
2. M. A. Marti-Renom, A. Stuart, A. Fiser, R. Sanchez, F. Melo and A. Sali, *Annu. Rev. Biomol. Struct.*, 2000, **29**, 291-325.
3. N. Eswar, M. A. Marti-Renom, B. Webb, M. S. Madhusudhan, D. Eramian, M. Shen, U. Pieper and A. Sali, *Current Protocols in Bioinformatics*, 2006, **15**, 1-30.
4. M. Kolbe, H. Besir, L. O. Essen and D. Oesterhelt, *Science*, 2000, **288**, 1390-1396.
5. M.-Y. Shen and A. Sali, *Protein Sci*, 2006, **15**, 2507-2524.

6. B. R. Brooks, R. E. Bruccoleri, B. D. Olafson, D. J. States, S. Swaminathan and M. Karplus, *J. Comput. Chem*, 1983, **4**, 187-217.
7. A. D. MacKerell Jr., D. Bashford, M. Bellot, R. L. Dunbrack, J. D. Evanseck, M. J. Field, S. Fischer, J. Gao, H. Guo, S. Ha, D. Joseph-McCarthy, L. Kuchnir, K. Kuczera, F. T. K. Lau, C. Mattos, S. Michnick, T. Ngo, D. T. Nguyen, B. Prodhom, W. E. I. Reiher, B. Roux, M. Schlenkrich, J. C. Smith, R. Stote, J. Straub, M. Watanabe, J. Wiorkiewicz-Kuczera, D. Yin and M. Karplus, *J. Phys. Chem. B*, 1998, **102**, 3586-3616.
8. A. D. MacKerell Jr., M. Feig and C. L. I. Brooks, *J. Comput. Chem*, 2004, **25**, 1400-1415.
9. E. Tajkhorshid, J. Baudry, K. Schulten and S. Suhai, *Biophys. J.*, 2000, **78**, 683-693.
10. A. D. Gruia, A.-N. Bondar, J. C. Smith and S. Fischer, *Structure*, 2005, **13**, 617-627.
11. C. del Val, L. Bondar and A.-N. Bondar, *J. Struct. Biol.*, 2014, **186**, 95-111.
12. L. A. Kelley and M. J. E. Sternberg, *Nature Protoc.*, 2009, **4**, 363-371.
13. C. del Val, J. Royuela-Flor, S. Milenkovic and A.-N. Bondar, *Biochim. Biophys. Acta Bioenergetics*, 2014, **1837**, 643-655.